ACS APPLIED MATERIALS & INTERFACES

Research Article

www.acsami.org

Structure-Specific Liquid Crystal Anchoring Induced by the Molecular Combing of Short Oligonucleotides

Saonti Chakraborty, Patrick S. Noonan, Jon Monserud, and Daniel K. Schwartz*

Department of Chemical and Biological Engineering University of Colorado Boulder, Boulder, Colorado 80309, United States

Supporting Information

ABSTRACT: Surface-immobilized oligonucleotides were "combed" by meniscus motion and exposed to a nematic liquid crystal (LC). Although the oligonucleotides were as short as 16 bases, they were apparently oriented by this process and, in turn, successfully biased the orientation of the adjacent LC material. Single-stranded DNA (ssDNA) induced LC orientation in the combing direction, while hybridized double-stranded DNA (dsDNA) rotated the azimuthal LC orientation by ~30° from the combing direction. The sensitivity of the chiral response to mixed ssDNA/dsDNA surfaces was characterized by employing complementary DNA that was longer than the immobilized DNA, resulting in single-stranded overhangs of various lengths. A rotated LC orientation was observed even when more than 70% of the DNA was single-stranded, and the transition from the rotated to nonrotated response was apparently discontinuous as a function of ssDNA surface coverage. These phenomena represent a sensitive DNA hybridization detection strategy that can potentially comprise a multiplexed assay.

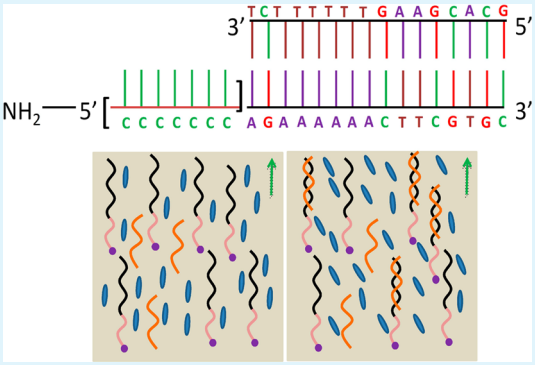

KEYWORDS: *liquid crystals, DNA, hybridization, heterogeneity, quantitative analysis, biosensor, azimuthal LC rotation*

INTRODUCTION

The extension of DNA by shear flow at a receding air−water interface (i.e., molecular combing) is often employed for genome mapping,[1,2] for DNA sequencing,[3] and in polymer physics research.[4−11] During molecular combing, shear flow in the neighboring aqueous phase and/or capillary forces associated with the three-phase line introduce stresses along the length of the DNA to extend it in a configuration with the long molecular axis perpendicular to the receding interface.[5] While alternative strategies for elongating DNA at interfaces have been demonstrated, including electrochemical,[12] opto-mechanical,[13] or hydrodynamic[14] methods, molecular combing is the simplest and most accessible approach. Furthermore, combined with an appropriate transduction strategy, molecular combing can be used in a label-free detection scheme. To date molecular combing applications have focused on DNA sequencing or genome mapping since they have required long (>kbp) polymeric DNA. A more robust detection strategy would be capable of detecting elongated *short* oligonucleotides (<50nt) and reproducibly distinguishing single-stranded DNA (ssDNA) from double-stranded DNA (dsDNA) as an assay for detecting DNA hybridization events. Such an approach would broaden the scope of applications that utilize the advantages of molecular combing to include clinical diagnostics, food safety monitoring, and biothreat detection. Here, we demonstrate that liquid crystals (LCs) can be used to identify elongated oligonucleotides in a DNA hybridization detection scheme.

The utility of liquid crystals as a transduction element has been demonstrated for translating a wide range of molecular binding events into a measurable signal. For example, binding events involving aptamers,[15,16] peptides,[17] enzymes,[18] and membrane receptors[16,19] that occur at liquid crystalline interfaces have been shown to induce changes to interfacial LC orientations. The optical anisotropy of LCs permits the orientation of liquid crystal molecules to be readily measured using polarized light.[20] LCs offer several advantages over alternative transduction strategies such as fluorescence, UV−vis, electrochemical, or mass-sensitive techniques. LC materials are inexpensive and require simple instrumentation compared with technologies required for traditional detection strategies. Due to their intrinsic elasticity, LC orientations propagate over macroscopic distances (μm), providing a natural amplification effect and increased sensitivity to stimuli. Thus, LCs offer an alternative transduction strategy that is attractive for point-of-use applications.

Recent studies have revealed that azimuthal LC orientation can be controlled using sheared or combed DNA.[21−23] In the later approach, genomic lambda phage dsDNA (λ-DNA) combed onto a [3-glycidoxypropyl] methyltriethoxysilane (GPTMS) self-assembled monolayer (SAM) induced azimuthal LC orientation ~30° from the combing direction. Interestingly the rotation of the LC alignment did not correlate with the major groove of DNA but apparently resulted from charge−dipole interactions between polar LC molecules and negative

Received: October 2, 2015
Accepted: November 12, 2015
Published: November 12, 2015

DOI: 10.1021/acsami.5b09335
ACS Appl. Mater. Interfaces 2015, 7, 26874−26879

charges along the phosphodiester backbone of DNA. When denatured lambda phage DNA (i.e., ssDNA) was instead combed onto the surface, the azimuthal LC orientation was parallel to the stretching direction. Thus, azimuthal LC orientations were used to distinguish between ssDNA and dsDNA, illustrating the potential for DNA based biosensing. The underlying GPTMS SAM promoted exquisite sensitivity since it possessed low azimuthal anchoring energy, allowing for microscopic perturbations induced by dsDNA to propagate over macroscopic distances. For example, it was shown that one dsDNA molecule could align upward of 10^{14} LC molecules, a sensitivity approaching single molecule detection.

This ability to detect specific DNA conformations (i.e., ssDNA vs dsDNA) via azimuthal LC orientation shows promise as an approach for a sensitive and selective detection strategy. However, in order for this detection scheme to be realized as a robust assay, short immobilized DNA (i.e., oligonucleotides) must be identified via azimuthal LC orientation. The λ-DNA utilized in the initial proof-of-concept study described above was ~48.5 kbps (approximately 16 μm as fully extended dsDNA) in length, while typical probes for detecting DNA hybridization (e.g., via PCR) are <100 bases long.[24] Hence, it is unclear whether the molecular fluctuations that occur during molecular combing would permit the combing of short DNA probes.

In the present study, we first evaluated the ability of immobilized combed oligonucleotides to induce azimuthal LC orientation in order to test whether azimuthal LC orientations can be exploited to detect DNA hybridization. We found that, analogous to previous work using λ-DNA that revealed DNA structure-specific azimuthal LC orientations,[22] surface immobilized and combed short oligonucleotides (ssDNA oligos) also induced azimuthal LC orientation in the stretching direction. When a complementary DNA strand was introduced to the aqueous phase prior to combing, hybridization with the surface-immobilized strand occurred and the azimuthal orientation after combing was rotated ~30° from the stretching direction. We evaluated the sensitivity of this approach by studying induced azimuthal LC orientation as a function of the fraction of ssDNA and dsDNA at the solid interface and studied the evolution of this response as a function of changing area fraction.

MATERIALS AND METHODS

Oligonucleotides. Figure 1 shows a schematic of the oligonucleotides used in this study. All oligonucleotides were purchased from Invitrogen. The "target" oligonucleotide strand used in our experiments was 16 bases long, whereas the "probe" strands used were amine-modified at the 5′-end and also of varying lengths. The "probe" lengths were modified by adding repetitive units of cytosine (C) as shown in Figure 1; the additional poly-C segments being n = 4, 8, 16, and 32 bases long. This additional segment was assumed to be unhybridized in the presence of the complementary "target" strand. The ratio of the length of this additional (ssDNA) segment to the total length of the DNA represented an unhybridized fraction, later denoted by F_{SS}. For example, for n = 8, $F_{SS} = 8/(16 + 8) = 0.33$. In the absence of any additional poly-C segment, the "probe" was fully complementary to the "target" strand and potentially resulted in complete hybridization (F_{SS} = 0, that is, purely dsDNA). Two other oligonucleotides, namely, noncomplementary and single-base mismatch DNA (as shown in Figure 1) were used in control experiments. For use during the experiments, ultrapure DNase/RNase free distilled water from ThermoFisher Scientific was used to make 125micromolar (μM) stock solution from the purchase lyophilized oligonucleotides and stored in 10microliter (μL) vials.

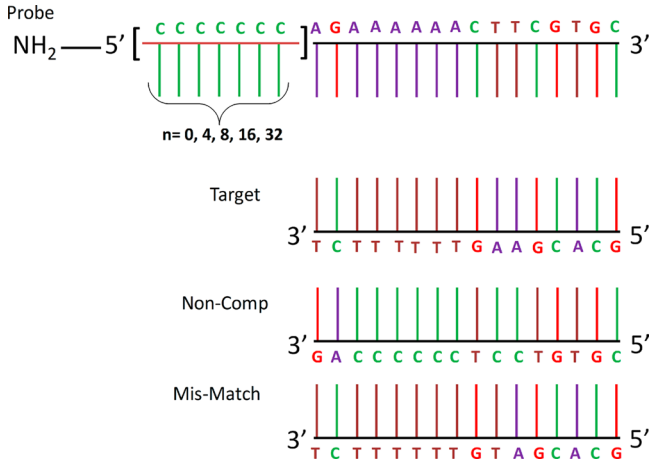

Figure 1. Schematic diagram of the oligonucleotides used in the study. Repetitive cytosine (C) units were added to the 16 base amine-terminated "probe" sequence to vary its length. The "target" sequence is complementary to the basic "probe" sequence. Non-Comp and Mis-Match sequences were used for control experiments.

Surface Preparation. We utilized an epoxide-amine ring opening reaction to covalently attach amine functionalized oligonucleotides to a monolayer of GPTMS deposited onto fused silica surfaces. GPTMS and octadecyltriethoxysilane (abbreviated as OTES) monolayers were prepared using a liquid phase deposition approach[25] on borosilicate glass slides using methods described briefly here and in greater detail in ref 12. The slides were sequentially cleaned with 2% aqueous micro-90 surfactant, deionized water (18.2MΩ), and piranha solution (30% aqueous hydrogen peroxide (H_2O_2) and concentrated sulfuric acid (H_2SO_4), both purchased from Fisher Scientific, 1:3 v/v) at 80 °C for 1 h. (***Warning:*** *piranha solution reacts strongly with organic compounds and should be handled with extreme caution.*) Following piranha cleaning, the slides were rinsed with deionized water, dried under an ultrapure N_2 stream, and cleaned using a UV-ozone exposure for ~1 h. For GPTMS deposition, cleaned slides were then placed in a deposition solution containing toluene, GPTMS, and *n*-butylamine in a 60:3:1 volume ratio for 60 min at room temperature. (Note: *n*-butylamine was added during the SAM deposition consistent with the amine-catalyzed approach to SAM deposition described by Walba et al.[26]) For OTES deposition, a similar deposition solution containing OTES (instead of GPTMS) was first heated to 60 °C before placing the clean glass slides in the deposition solution. After incubating for ~1 h, all slides were rinsed with toluene, dried under an ultrapure N_2 stream, and stored in a vacuum desiccator. Efficient monolayer deposition was verified using the static sessile drop method on a custom built contact angle goniometer (contact angle $\theta_C \approx 52°$ for GPTMS and $\theta_C \geq 90°$ for OTES).

Oligonucleotide Deposition and Combing. The amine-modified oligonucleotides were dissolved in 1× PBS (pH > 8.0) at ~20 nM concentration. GPTMS modified substrates were then immersed in the deposition solution and incubated overnight to allow sufficient time for the amine groups to react with the surface immobilized epoxide groups. The oligonucleotides were deposited onto GPTMS-modified substrates by exploiting the fact that amine groups react readily with epoxides at elevated pH.[27] The success of the deposition was verified by using fluorescently labeled oligonucleotides and capturing a total internal reflection fluorescence microscope (TIRFM) image of the surface after deposition A representative TIRFM image of a GPTMS surface with covalently attached Alexa Flour 488 modified oligonucleotides is shown in Figure S1 of the Supporting Information. From images such as these, we estimated the surface coverage of DNA to be ~14 oligos/μm^2. We used these same deposition conditions throughout our experiments to maintain an approximately constant surface coverage of DNA.

DOI: 10.1021/acsami.5b09335
ACS Appl. Mater. Interfaces 2015, 7, 26874−26879

The combing of oligonucleotide-modified GPTMS surfaces was performed in a controlled direction using an inverted linear dipper at a controlled speed of 1 mm/min. For control experiments without hybridized dsDNA (F_{SS} = 1), the combing was done after removing the surfaces from the deposition solution containing "probe" oligonucleotide. In all other cases, probe-decorated surfaces were removed from the deposition solution containing "probe" oligonucleotide, rinsed with water and then incubated in a second deposition solution with the "target" oligonucleotide (complementary, noncomplementary, or mismatch) for ∼1 h prior to combing. Finally, nematic LC 4-cyano-4′-pentylbiphenyl (5CB) was confined in a sandwich cell comprising an OTES-treated glass surface (for uniform homeotropic alignment) and the oligonucleotide-functionalized substrate. The thickness of the cell was maintained at ∼25 μm using Mylar spacers between the two substrates. 5CB was loaded into the cell by heating to ∼40 °C (where 5CB is isotropic) and then drawn between the two substrates.

Analysis of Orientation Using Polarized Microscopy. LC orientation was determined by analyzing the polarized light micrographs obtained using a custom transmission microscope. Sequences of images were obtained for various angles (ϕ) in the range 0–90° between the combing direction and the analyzer, while keeping the analyzer and polarizer crossed with respect to one another (indicated in Figure S2). Since extinction observed in these cross-polarized images arose from azimuthal (in-plane) alignment of the LC molecules parallel to either the polarizer or the analyzer, the images were analyzed to find the most probable extinction angle and, hence, the orientation of the LC molecules with respect to the combing direction.

To quantify extinction, the average transmitted light intensity was calculated from the individual pixel intensities of an image, averaged over all pixels in the image and then plotted as a function of ϕ. This was performed for each sequence of images using a customized Mathematica based algorithm. The resulting plot of transmitted intensity as a function of ϕ was analyzed using

$$I_r = \sin^2(2\phi) \quad (1)$$

where I_r was the transmitted normalized intensity. For instance, when the azimuthal director was aligned with the stretching direction, the intensity was minimized when ϕ was equal to 0° or 90°.

RESULTS

A cartoon of the stretched oligonucleotides on the GPTMS surface is shown in Figure 2, indicating immobilized amine-modified probe ssDNA, double-stranded (hybridized) segments, and the resulting LC alignment. The azimuthal orientation of the LCs is shown with respect to the combing direction (green arrow). In addition to the hybridized DNA, it is assumed that some strands of unhybridized "probe" (ssDNA) well as nonspecifically adsorbed "target" DNA are also generally present on the surface. As described above, combing was achieved using a receding air–water interface, and sandwich LC cells were constructed using the DNA-laden surface and an OTES-surface, which induced homeotropic orientation. In control experiments without any DNA, where a GPTMS surface was exposed to a receding air–water interface, polarized light images consistently showed random azimuthal orientation.[22]

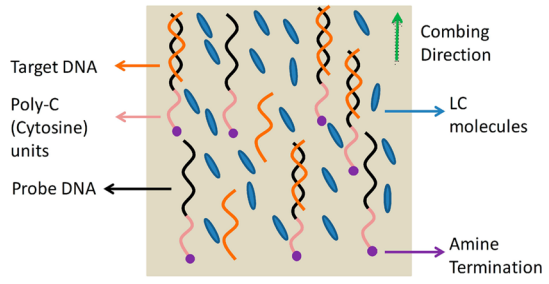

Figure 2. Schematic representation showing the hybridization of immobilized and combed "probe" DNA strands and the resulting LC orientation with respect to the combing direction. The cartoon also shows unhybridized and nonspecifically adsorbed DNA strands that account for the nonuniform background in the optical micrographs shown in Figure 3.

Oligonucleotide Induced LC Orientation. We observed that short immobilized DNA oligonucleotides were in fact capable of inducing azimuthal LC orientation when combed onto a solid substrate. When ssDNA was immobilized and combed on a GPTMS substrate, we consistently observed azimuthal LC orientation parallel with the stretching direction. This is demonstrated in Figure 3a-I, where a dark image

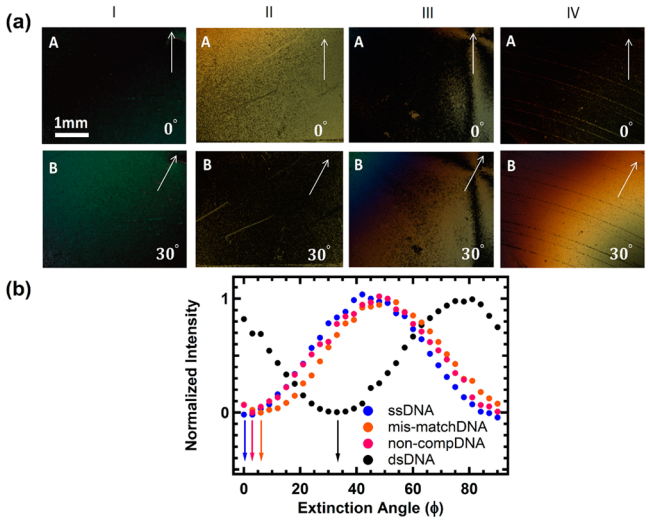

Figure 3. (a) Polarized light microscope images of hybrid LC cells made with GPTMS and OTES monolayers containing (I) ssDNA, (II) dsDNA, (III) ssDNA, and noncomplementary DNA and (IV) ssDNA and single-base mismatch DNA. Top row images (panels I–IVA) were obtained when the angle between the combing direction and analyzer was 0°. Bottom row images (panels I–IVB) show the same sample region when the angle between the combing direction and analyzer was 30°. White arrows indicate the combing direction. The long bright "lines" in the images appear from scratches on the substrate surface or a as a result of dust stuck to the surface. (b) Normalized transmitted intensity as a function of ϕ, averaged over all image pixels.

indicates low light transmission through crossed polarizers at an angle of ϕ = 0° (Figure 3a-I-A) and a bright image indicates high transmission through crossed polarizers at an angle of ϕ = 30° (Figure 3a-I-B); these observations are consistent with LC orientation parallel to the combing direction. When a complementary target DNA strand was added to the aqueous phase prior to combing, DNA hybridization occurred with the surface immobilized NH-probe, and the azimuthal orientation of the LC director was found to be ∼30° with respect to the combing direction (Figure 3a-II-A and B). As control experiments, optical images through crossed polarizers were obtained for LC cells when the complementary target DNA strand in the aqueous phase was replaced by noncomplementary (Figure 3a-III) or single base mismatch (Figure 3a-IV) target DNA strands, respectively. In both cases, ssDNA apparently failed to hybridize and the most probable extinction direction was found to lie along the stretching direction.

DOI: 10.1021/acsami.5b09335
ACS Appl. Mater. Interfaces 2015, 7, 26874–26879

In order to quantitatively determine the LC alignment angle, we measured the transmitted optical intensity as a function of ϕ and plotted the variation of intensity as shown in Figure 3b. Four replicate samples were tested for each type of target and their polarized optical images obtained in order to measure the LC alignment angle (using eq 1). By comparing the plots, one can see that the LC alignment (minimum intensity) in the presence of ssDNA was consistent with $\phi \sim 0°$ and did not change appreciably in the cases of noncomplementary or mismatch DNA. In the presence of dsDNA, however, LC alignment was consistent with $\phi \sim 33°$. Again, these measurements suggested that combed oligonucleotides were capable of inducing azimuthal LC orientation. To our knowledge, this is the first example demonstrating molecular combing of polymers on this length scale (contour length <100 nm). The lack of previous reports using short polymers is presumably due to an insufficiently sensitive analytical technique for measuring their elongation.[6] However, LC orientation is extraordinarily sensitive to subtle broken symmetries, and is apparently sensitive enough to measure the results of this combing. A detailed sequence of polarized optical micrographs for various angles ϕ in the range 0−90° is shown in Figure S3.

In an effort to better understand the azimuthal LC orientation associated with ssDNA and dsDNA, we systematically varied the relative fractions of ssDNA and dsDNA present at the interface. We achieved this by varying the length of the probe DNA by adding repetitive units of cytosine, as discussed earlier. This poly-C segment was not complementary to any target DNA added and, therefore, represented a way to control the amount of ssDNA, even following incubation with complementary target. However, the fraction of the ssDNA due to the poly-C segments is actually best considered a lower limit, since it is likely that additional ssDNA was generally present as a result of nonspecifically adsorbed target and/or unhybridized immobilized probe. We represent our subsequent data as a function of F_{SS}, which as defined above, was calculated as the ratio of the length of the unhybridized portion of the probe DNA to the total probe length.

Figures 4a and S4 show representative polarized optical images for the various probe lengths. Four independent samples were tested for each length, and their polarized optical images obtained in order to measure the LC alignment angle (using eq 1). The mean values of the alignment angle were calculated and plotted as a function of F_{SS} in Figure 4b. The most probable extinction angle was found to be ∼30° for the entire range of lengths tested, and no particular trend was observed. This, together with the fact that the most probable extinction angle for samples containing only ssDNA (Fss = 1) was found to be ∼0°, suggested that the LC alignment exhibited a discontinuous transition as a function of F_{SS},[28] analogous to discontinuous transitions observed for homeotropic to planar anchoring.[29]

Although Figure 4b reveals that the average alignment angle was concentrated near 30° in the presence of additional ssDNA segments, we also found significant scatter in the LC orientation from sample to sample. These variations were sometimes larger than the experimental error associated with our ability to measure the relative alignment angle between DNA and LC. Since the alignment angle was determined by comparing macroscopic images to the nominal combing angle, these uncertainties may have resulted from small variations in local DNA orientation.

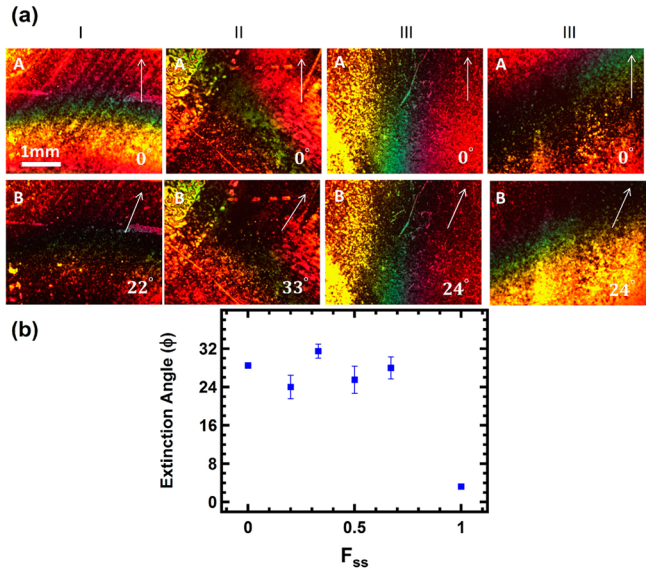

Figure 4. (a) Polarized light microscopy images of the hybrid LC cells made with GPTMS and OTES monolayers for varying F_{SS}. (I) F_{SS} = 0.2, (II) F_{SS} = 0.33, (III) F_{SS} = 0.5, and (IV) F_{SS} = 0.67. Upper row (panels I−IVA) shows the images for unrotated crossed polarizers. Images in the bottom row (panels I−IVB) were obtained at the angle of rotation where maximum extinction occurred (referred to below as ϕ_{min}). These images show that regions of extinction corresponding to hybridized DNA existed for all fractions. White arrows indicate the direction of molecular combing. (b) Plot of the most probable extinction angle as a function of the (lower limit) fraction of unhybridized DNA.

Test of Sensitivity. As an essential step toward understanding the azimuthal orientation associated with ssDNA and dsDNA and developing a robust sensor strategy for detecting hybridization events, we investigated the minimum concentration of the fully complementary "target" required to detect the hybridization. For this test of sensitivity, the target concentration was systematically varied in the range of 1 pM to 100 nM, and the mean extinction angle corresponding to each concentration was determined. Over this range of target concentration, the extinction angle was typically in the range 25−30° with no apparent trend with concentration. This placed an upper limit on the ultimate sensitivity of this approach at a value of 1 pM (∼10^9 target oligos) and suggested that the response was relatively insensitive to concentration over this range. Therefore, the remainder of the experiments reported here were performed at a target concentration of ∼20 nM, because at this concentration, it was easier to handle the very small volumes required.

Heterogeneity. In order to quantify the heterogeneity in the images at a particular angle ϕ, we used customized algorithms written in the Mathematica programming environment to find a correlation coefficient between the intensity profile of every pixel within a series of images taken at varying ϕ and the theoretical profile associated with eq 1. The correlation coefficient was maximized when the azimuthal orientation was parallel with the analyzer (i.e., extinction), allowing us to define the azimuthal director for each pixel. Since this was done for every pixel, we counted the number of pixels with a particular extinction angle and divided this by the total pixel count to find the spatial probability for alignment/extinction at a particular angle.

DOI: 10.1021/acsami.5b09335
ACS Appl. Mater. Interfaces 2015, 7, 26874−26879

For illustration, the distributions of alignment angles for two cases, namely, F_{SS} = 0.5 and F_{SS} = 0.67, are shown in Figure 5a

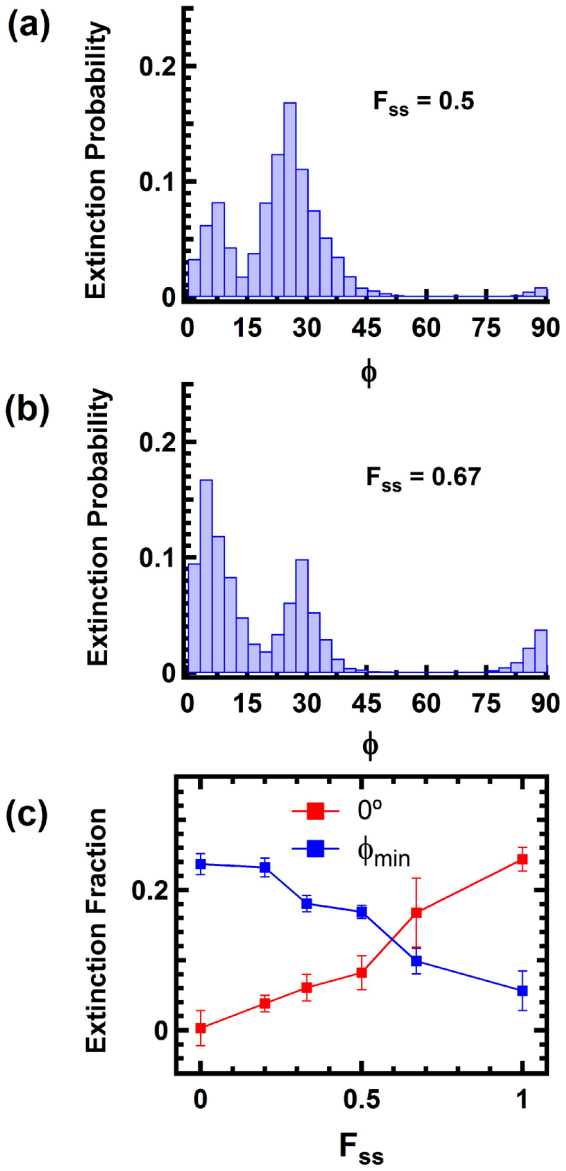

Figure 5. Histograms showing the spatial probability of alignment/extinction as a function of the combing direction with respect to the analyzer for (a) F_{SS} = 0.5 and (b) F_{SS} = 0.67. (c) Plot showing the peak areas associated with alignment/extinction at ϕ = 0° (red markers) and $\phi = \phi_{min}$ (blue markers) as a function of F_{SS}.

and b, respectively. In both cases, two peaks were observed, one near ϕ = 0° and the other near ϕ = 30°. Similar plots showing the probability distributions of extinction are given for all values of F_{SS} (including pure ssDNA and dsDNA) in Figure S5. These distributions of alignment angle suggest that subtle spatial heterogeneity led to a situation where some regions of the surface promoted alignment at ~30° and other regions caused alignment in the combing direction (0°). The relative magnitudes of the two peaks change systematically with F_{SS}; however, we did not observe the appearance of peaks at intermediate angles nor a systematic shift in peak position with F_{SS}. This again suggested that the transition between LC alignment at these two angles was discontinuous with respect to F_{SS}, and that the heterogeneity reflected spatial variation of F_{SS} about the critical value for the transition.

To quantify the systematic change in the magnitudes of the two peaks, the areas under each of the two peaks were calculated and plotted in Figure 5c as a function of F_{SS}. From this graph, we see that in the case of F_{SS} = 1 (pure ssDNA) and F_{SS} = 0 (pure dsDNA), extinction was observed primarily at only one angle: ϕ = 0° and ϕ = 30°, respectively. For intermediate values of F_{SS}, at least two subpopulations of spatial regions, each characterized by a distinct LC alignment with respect to the combing direction, coexisted at the solid surface, and the relative fractions of these two populations evolved systematically with F_{SS}.

The presence of these coexisting spatial populations could originate from local variations in the actual fraction of ssDNA due, for example, to the nonuniform presence of nonspecifically adsorbed unhybridized target DNA strands. This may explain the nonuniformity observed in Figure 4 and the relatively large scatter associated with the extinction angles shown in Figure 4b. Interestingly, this spatial variability also emphasized the incredible sensitivity of LC alignment to small changes in surface structure, where subtle differences in the relative amount of ssDNA and dsDNA presumably cause a discontinuous and dramatic change in LC azimuthal orientation.

CONCLUSIONS

While molecular combing via meniscus motion has frequently been used to extend/orient large polymers, it is intuitively surprising that small oligonucleotides can be successfully oriented by this crude process. Interestingly, because these molecules were small and sparsely decorated on the surface, the characterization of their orientation was itself fundamentally challenging, and uniquely enabled by the extraordinary sensitivity of nematic LCs to subtle broken symmetries. Additionally, the specific azimuthal orientation promoted by the combed DNA was sensitive to the DNA conformation and provided a direct signature of hybridization. This, along with the fact that the extent of alignment signature of DNA hybridization was relatively insensitive to the presence of large amounts of unhybridized ssDNA, suggests that this phenomenon can potentially be exploited to design a sensitive scheme for the detection of DNA hybridization. Here, we found that the distinctive LC response to dsDNA was unperturbed even when more than 70% of the DNA remained single-stranded. It would certainly be interesting to develop new methods that could extend this measurement to even larger fractions of ssDNA interference to clarify how much ssDNA can be tolerated when trying to identify low surface coverage of dsDNA.

ASSOCIATED CONTENT

Supporting Information

The Supporting Information is available free of charge on the ACS Publications website at DOI: 10.1021/acsami.5b09335.

A representative TIRFM image of a GPTMS surface with covalently attached Alexa Fluor 488 modified oligonucleotides. Also included are Polarized Light Microscopy images of hybrid aligned LC cells containing unhybridized DNA, and hybridized DNA with various probe lengths, and distributions of dark pixels for varying probe DNA lengths (PDF)

DOI: 10.1021/acsami.5b09335
ACS Appl. Mater. Interfaces 2015, 7, 26874−26879

AUTHOR INFORMATION

Corresponding Author

*E-mail: daniel.schwartz@colorado.edu.

Notes

The authors declare no competing financial interest.

ACKNOWLEDGMENTS

The authors gratefully acknowledge support from the National Science Foundation award #CBET-1160202 and from the Soft Materials Research Center (NSF-MRSEC DMR 1420736).

REFERENCES

(1) Michalet, X.; Ekong, R.; Fougerousse, F. o.; Rousseaux, S.; Schurra, C.; Hornigold, N.; Slegtenhorst, M. v.; Wolfe, J.; Povey, S.; Beckmann, J. S.; Bensimon, A. Dynamic Molecular Combing: Stretching the Whole Human Genome for High-Resolution Studies. *Science* **1997**, *277* (5331), 1518−1523.

(2) Lebofsky, R.; Bensimon, A. Single DNA molecule analysis: Applications of molecular combing. *Briefings Funct. Genomics Proteomics* **2003**, *1* (4), 385−396.

(3) Xu, M.; Fujita, D.; Hanagata, N. Perspectives and Challenges of Emerging Single-Molecule DNA Sequencing Technologies. *Small* **2009**, *5* (23), 2638−2649.

(4) Bensimon, A.; Simon, A.; Chiffaudel, A.; Croquette, V.; Heslot, F.; Bensimon, D. Alignment and sensitive detection of DNA by a moving interface. *Science* **1994**, *265* (5181), 2096−8.

(5) Bensimon, D.; Simon, A. J.; Croquette, V.; Bensimon, A. Stretching DNA with a Receding Meniscus - Experiments and Models. *Phys. Rev. Lett.* **1995**, *74* (23), 4754−4757.

(6) Marko, J. F.; Siggia, E. D. Stretching DNA. *Macromolecules* **1995**, *28* (26), 8759−8770.

(7) Smith, D. E.; Babcock, H. P.; Chu, S. Single-Polymer Dynamics in Steady Shear Flow. *Science* **1999**, *283* (5408), 1724−1727.

(8) Bustamante, C.; Smith, S. B.; Liphardt, J.; Smith, D. Single-molecule studies of DNA mechanics. *Curr. Opin. Struct. Biol.* **2000**, *10* (3), 279−285.

(9) Schroeder, C. M.; Babcock, H. P.; Shaqfeh, E. S. G.; Chu, S. Observation of Polymer Conformation Hysteresis in Extensional Flow. *Science* **2003**, *301* (5639), 1515−1519.

(10) Chan, T. F.; Ha, C.; Phong, A.; Cai, D.; Wan, E.; Leung, L.; Kwok, P. Y.; Xiao, M. A simple DNA stretching method for fluorescence imaging of single DNA molecules. *Nucleic Acids Res.* **2006**, *34* (17), e113.

(11) van Mameren, J.; Gross, P.; Farge, G.; Hooijman, P.; Modesti, M.; Falkenberg, M.; Wuite, G. J. L.; Peterman, E. J. G. Unraveling the structure of DNA during overstretching by using multicolor, single-molecule fluorescence imaging. *Proc. Natl. Acad. Sci. U. S. A.* **2009**, *106* (43), 18231−18236.

(12) Schwartz, D. C.; Koval, M. Conformational dynamics of individual DNA molecules during gel electrophoresis. *Nature* **1989**, *338* (6215), 520−522.

(13) Gross, P.; Laurens, N.; Oddershede, L. B.; Bockelmann, U.; Peterman, E. J. G.; Wuite, G. J. L. Quantifying how DNA stretches, melts and changes twist under tension. *Nat. Phys.* **2011**, *7* (9), 731−736.

(14) Petit, C. A. P.; Carbeck, J. D. Combing of molecules in microchannels (COMMIC): A method for micropatterning and orienting stretched molecules of DNA on a surface. *Nano Lett.* **2003**, *3* (8), 1141−1146.

(15) Noonan, P. S.; Roberts, R. H.; Schwartz, D. K. Liquid Crystal Reorientation Induced by Aptamer Conformational Changes. *J. Am. Chem. Soc.* **2013**, *135* (13), 5183−5189.

(16) Noonan, P. S.; Mohan, P.; Goodwin, A. P.; Schwartz, D. K. DNA Hybridization-Mediated Liposome Fusion at the Aqueous Liquid Crystal Interface. *Adv. Funct. Mater.* **2014**, *24* (21), 3206−3212.

(17) Park, J. S.; Teren, S.; Tepp, W. H.; Beebe, D. J.; Johnson, E. A.; Abbott, N. L. Formation of oligopeptide-based polymeric membranes at interfaces between aqueous phases and thermotropic liquid crystals. *Chem. Mater.* **2006**, *18* (26), 6147−6151.

(18) Brake, J. M.; Daschner, M. K.; Luk, Y. Y.; Abbott, N. L. Biomolecular interactions at phospholipid-decorated surfaces of liquid crystals. *Science* **2003**, *302* (5653), 2094−2097.

(19) Tan, L. N.; Orler, V. J.; Abbott, N. L. Ordering Transitions Triggered by Specific Binding of Vesicles to Protein-Decorated Interfaces of Thermotropic Liquid Crystals. *Langmuir* **2012**, *28* (15), 6364−6376.

(20) Miller, D. S.; Carlton, R. J.; Mushenheim, P. C.; Abbott, N. L. Introduction to Optical Methods for Characterizing Liquid Crystals at Interfaces. *Langmuir* **2013**, *29* (10), 3154−3169.

(21) Cha, Y. J.; Gim, M.-J.; Oh, K.; Yoon, D. K. In-Plane Switching Mode for Liquid Crystal Displays Using a DNA Alignment Layer. *ACS Appl. Mater. Interfaces* **2015**, *7* (24), 13627−13632.

(22) Malone, S. M.; Schwartz, D. K. Macroscopic Liquid Crystal Response to Isolated DNA Helices. *Langmuir* **2011**, *27* (19), 11767−11772.

(23) Nakata, M.; Zanchetta, G.; Buscaglia, M.; Bellini, T.; Clark, N. A. Liquid crystal alignment on a chiral surface: Interfacial interaction with sheared DNA films. *Langmuir* **2008**, *24* (18), 10390−10394.

(24) Heller, M. J. DNA microarray technology: Devices, systems, and applications. *Annu. Rev. Biomed. Eng.* **2002**, *4*, 129−153.

(25) Tsukruk, V. V.; Luzinov, I.; Julthongpiput, D. Sticky Molecular Surfaces: Epoxysilane Self-Assembled Monolayers. *Langmuir* **1999**, *15* (9), 3029−3032.

(26) Walba, D. M.; Liberko, C. A.; Korblova, E.; Farrow, M.; Furtak, T. E.; Chow, B. C.; Schwartz, D. K.; Freeman, A. S.; Douglas, K.; Williams, S. D.; Klittnick, A. F.; Clark, N. A. Self-assembled monolayers for liquid crystal alignment: simple preparation on glass using alkyltrialkoxysilanes. *Liq. Cryst.* **2004**, *31* (4), 481−489.

(27) Taylor, S.; Smith, S.; Windle, B.; Guiseppi-Elie, A. Impact of surface chemistry and blocking strategies on DNA microarrays. *Nucleic Acids Res.* **2003**, *31* (16), e87.

(28) Shioda, T.; Wen, B.; Rosenblatt, C. Continuous nematic anchoring transition due to surface-induced smectic order. *Phys. Rev. E: Stat. Phys., Plasmas, Fluids, Relat. Interdiscip. Top.* **2003**, *67* (4), 041706.

(29) Price, A. D.; Schwartz, D. K. Anchoring of a nematic liquid crystal on a wettability gradient. *Langmuir* **2006**, *22* (23), 9753−9759.

DOI: 10.1021/acsami.5b09335
ACS Appl. Mater. Interfaces 2015, 7, 26874−26879